ИЗВЕСТИЯ ВЫСШИХ УЧЕБНЫХ ЗАВЕДЕНИЙ.
Т 69 (8) Серия «**ХИМИЯ И ХИМИЧЕСКАЯ ТЕХНОЛОГИЯ**» 2026
V 69 (8) **ChemChemTech** 2026

DOI: 10.6060/ivkkt.20266908.7137
УДК: 546.05+54.057: 549.731.11

ТРИ ВАРИАНТА СИНТЕЗА НИКЕЛЬАЛЮМИНАТНОЙ ШПИНЕЛИ С ИСПОЛЬЗОВАНИЕМ ПРОДУКТОВ ГОРЕНИЯ КСЕРОГЕЛЕЙ. ЧАСТЬ 2

Н.В. Филатова, А.С. Артюшин, Н.Ф. Косенко, А.Г. Никандрова

Наталья Владимировна Филатова (ORCID 0000-0001-7552-3496)*, Артем Сергеевич Артюшин, Надежда Федоровна Косенко (ORCID 0000-0001-8806-7530), Анна Геннадьевна Никандрова

Кафедра технологии керамики и электрохимических производств, Ивановский государственный химико-технологический университет, пр. Шереметевский, 7, Иваново, Российская Федерация, 153000
E-mail: zyanata@mail.ru*, artyushin_as@mail.ru, nfkosenko@gmail.com, annanikandrova579@gmail.com

Методом горения были получены продукты горения ксерогеля (ПГК) алюмооксидного и никельалюминатного состава с использованием лимонной кислоты (ЛК) в качестве топлива. Описаны свойства ПГК, определенные методами рентгенофазового, термического, ИК-спектрального анализа, сканирующей электронной микроскопии и др. Методом рентгенофазового анализа установлено, что горение стехиометрической смеси нитрата алюминия с ЛК приводило к образованию рентгеноаморфного продукта, который кристаллизовался с образованием γ-Al_2O_3 при термообработке (700-900 °С), переходившей затем (1100 °С) в α-Al_2O_3. Признаки $NiAl_2O_4$ обнаруживались в as-prepared ПГК. С помощью инфракрасного пирометра установлены максимальные температуры горения: 429 и 468 °С для ПГК алюмооксидного и никельалюминатного состава соответственно. Характер зависимостей температуры от времени для различных ПГК был аналогичным. Выполнен термический анализ ПГК. Определен состав газов, выделяющихся в ходе горения. Масс-спектральные кривые свидетельствовали о преимущественном выделении газообразных продуктов, соответствовавших уравнениям окислительно-восстановительных реакций: H_2O, N_2, CO_2. Приведен предположительный перечень уравнений реакций, приводивших к образованию шпинели. По ИК спектрам сделано предположение, что ПГК никельалюминатного состава (без отжига и после отжига) представлял собой частично инвертированную шпинель. Данные по низкотемпературной адсорбции азота свидетельствовали о незначительном уменьшении удельной площади поверхности ПГК (на 13-1%) и увеличении размеров кристаллитов (на 13-27%) в результате термообработки при 700 °С. Более высокая температура отжига (1100 °С) приводила к существенному сокращению межфазной поверхности (в 4-5 раз).

Ключевые слова: синтез горением растворов (ксерогелей), состав смеси для горения, оксид алюминия, никельалюминатная шпинель, продукт горения ксерогеля, отжиг продукта

THREE VARIANTS OF NICKEL ALUMINATE SPINEL SYNTHESIS USING XEROGEL COMBUSTION PRODUCTS. PART 2

N.V. Filatova, A.S. Artyushin, N.F. Kosenko, A.G. Nikandrova

Natalya V. Filatova (ORCID 0000-0001-7552-3496)*, Artyom S. Artyushin, Nadezhda F. Kosenko (ORCID 0000-0001-8806-7530), Anna G. Nikandrova

Department of Ceramics Technology and Electrochemical Production, Ivanovo State University of Chemistry and Technology, Sheremetevskiy ave., 7, Ivanovo, 153000, Russia
E-mail: zyanata@mail.ru*, artyushin_as@mail.ru, nfkosenko@gmail.com, annanikandrova579@gmail.com

Combustion products of xerogel (XCPs) of alumina and nickel aluminate composition were obtained by combustion using citric acid (CA) as fuel. The XCP properties determined by the methods of X-ray diffraction, thermal, IR spectral analysis, scanning electron microscopy, etc. are described. By diffractometry, it was established that the combustion of a stoichiometric mixture of aluminum nitrate with CA led to the formation of an X-ray amorphous product, which crystallized to form γ-Al_2O_3 during heat treatment (700-900 °C), which then passed (1100 °C) into α-Al_2O_3. $NiAl_2O_4$ signs were found in as-prepared XCP. Using an infrared pyrometer, the maximum combustion temperatures were established: 429 and 468 °C for XCPs of alumina and nickel aluminate composition, respectively. The nature of temperature-time dependencies for different XCPs was similar. A thermal analysis of XCP was performed. The composition of gases released during combustion has been determined. The mass-spectral curves testified to the predominant emission of gaseous products that corresponded to the equations of redox reactions: H_2O, N_2, and CO_2. A hypothetical list of equations of reactions leading to the spinel formation is given. Based on the IR spectra, it was assumed that the nickel-aluminate XCPs (without annealing and after it) was a partially inverted spinel. The data on low-temperature nitrogen adsorption showed a slight decrease in the XCP specific surface area (by 13-19%) and an increase in the size of crystallites (by 13-27%) as a result of heat treatment at 700 °C. A higher annealing temperature (1100 °C) led to a significant reduction in the interfacial surface (4-5 times).

Keywords: solution (xerogel) combustion synthesis, combustion mixture composition, alumina, nickel aluminate spinel, xerogel combustion product, product annealing

Для цитирования:
Филатова Н.В., Артюшин А.С., Косенко Н.Ф., Никандрова А.Г. Три варианта синтеза никельалюминатной шпинели с использованием продуктов горения ксерогелей. Часть 2. *Изв. вузов. Химия и хим. технология*. 2026. Т. 69. Вып. 8. С. 116–123. DOI: 10.6060/ivkkt.20266908.7137.

For citation:
Filatova N.V., Artyushin A.S., Kosenko N.F., Nikandrova A.G. Three variants of nickel aluminate spinel synthesis using xerogel combustion products. Part 2. *ChemChemTech* [*Izv. Vyssh. Uchebn. Zaved. Khim. Khim. Tekhnol.*]. 2026. V. 69. N 8. P. 116–123. DOI: 10.6060/ivkkt.20266908.7137.

INTRODUCTION

This article is a logical continuation of the article [1], which substantiated 3 ways of synthesis of $NiAl_2O_4$ using xerogel combustion products (XCP) and described the production and properties of XCP of nickel oxide composition.

Aluminum oxide synthesized by combustion was characterized in pioneering work [2] along with other aluminate compounds ($MgAl_2O_4$, $CaAl_2O_4$, $Y_3Al_5O_{12}$ (YAG), β′-Al_2O_3, $LaAlO_3$ and ruby powder (Cr^{3+}-Al_2O_3)). In this work, for the first time, the synthesis of α-Al_2O_3 has been carried out at a low temperature (500 °C) by the burning a mixture of metal nitrate ($Al(NO_3)_3 \cdot 9H_2O$) with urea N_2H_4CO as fuel for a time of less than 5 min. The reaction was initiated by heating in a muffle furnace. As a result, hexagonal crystals α-Al_2O_3 with dimensions of 0.2-0.8 μm with a specific surface area of 8.3 m^2/g were obtained. The interest in aluminate compounds is understandable and is due to their great practical importance. Using the combustion method, various modifications of alumina were obtained: α- [2-8], γ- [9-12], β- [13, 14]. As a rule, aluminum nitrate served as an oxidizer in such a reaction, but metal formate was used in the work [6]. In the work [9], a complex of aluminum (III) with Schiff bases was used in the presence and absence of carbamide and glycine.

The reducing agent can be various organic compounds that form chelated complexes with di- and trivalent d-metals (Fig. 1), which increases the homogeneity of the reacting mixture, prevents segregation and precipitation during evaporation in order to obtain xerogel, and initiates a combustion reaction at low ignition temperatures.

In most studies, the authors chose urea $(NH_2)_2CO$ [2-5, 8, 13], glycine $C_2H_5NO_2$ [4, 7, 13], and citric acid [11, 13, 16]. In the review [17], it was noted that the use of urea, hydrazine N_2H_4, or carbohydrazide CH_6N_4O as fuel made it possible to obtain a single-phase product in the form of α-Al_2O_3, while the choice of glycine $C_2H_5NO_2$, acetylacetone $C_5H_8O_2$ or citric acid $C_6H_8O_7$ led to the formation of an amorphous powder, which, after annealing above 1100 °C, was transformed

into α-Al_2O_3. Zhuravlev *et al.* [8] using the example of the urea system, showed that the crystallization degree of the combustion product depended to a large extent on the molar ratio of fuel : oxidizer φ. For φ = 1.0-1.2, the researchers obtained a well-crystallized product, while the lack of fuel (φ = 0.6) led to the formation of an X-ray amorphous substance.

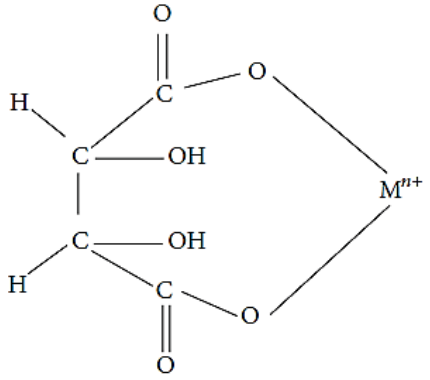

Рис. 1. Хелат между комплексообразующими катионами и лимонной кислотой [15]
Fig. 1. Chelate between complexing cations and citric acid [15]

A number of authors used mixed fuels: urea-glycine [18], urea-glycine-hexamethylenetetramine [10], urea-camphor [19], urea-citric acid [11].

Earlier [20], we synthesized Al_2O_3 using succinic acid. The xerogel combustion product (XCP) was amorphous up to 700 °C. Heat treatment at 900 °C led to the formation of crystalline γ-Al_2O_3, and higher temperature treatment (1100 °C) contributed to the formation of a well-crystallized single-phase product in the form of α-form. The size of the crystallites was 38.3 nm. XCP was composed of unevenly granular agglomerates of sharp-angled particles with a size of ~2 to ~10 μm. Its high reactivity was shown [21].

The combustion method is actively used to obtain various spinels, including $NiAl_2O_4$ [22-27]. In recent years, the combustion method has been in demand for the production of Ni-containing catalysts and their supporters of various compositions: Ni/Al_2O_3 [28-32], NiO/Al_2O_3 [33], Ni-$NiAl_2O_4$ [34], as well as $NiAl_2O_4$/NiO composites [35]. This is caused by the spinel stability, resistance to acids and alkalis, high melting point. The review [36] showed that $NiAl_2O_4$ was formed in the process of combustion, especially at elevated temperatures, or annealing (500-900 °C). X-ray diffraction confirmed the coexistence of the NiO and $NiAl_2O_4$ phases and the absence of alumina, which indicated the complete inclusion of aluminum in the spinel structure. Annealing above 800 °C contributed to the crystallization of the stable phase of $NiAl_2O_4$, in which nickel was evenly distributed. Subsequent spinel reduction led to the formation of Ni/Al_2O_3 catalysts with fine particles of Ni (10-30 nm), providing increased activity at moderate reaction temperatures. For this purpose, traditional fuels, in particular urea, are used [23, 26, 27]. The use of plant extract was original [24].

This part of the paper presents the results of the study of xerogel combustion products (XCP) obtained from nitrates and citric acid (CA), leading to the formation of alumina and nickel-aluminate spinel.

MATERIALS AND EXPERIMENTS

Used for synthesis reagents: aluminum nitrate (AN) $Al(NO_3)_3 \cdot 9H_2O$, nickel nitrate (NN) $Ni(NO_3)_2 \cdot 6H_2O$, citric acid $C_6H_8O_7 \cdot H_2O$ [HOOC-CH_2-C(OH)COOH-CH_2COOH] analytically pure.

To obtain XCP (A) and XCP (NA), respectively:

1) AN crystal hydrate taken as oxidizer and CA (fuel) according to the reaction equation:

$$6[Al(NO_3)_3 \cdot 9H_2O] + 5C_6H_8O_7 = 3Al_2O_3 + 9N_2 + 30CO_2 + 74H_2O;$$

2) NN and AN crystal hydrates (oxidizers) and CA (reducing agent) according to the reaction equation:

$$2[Ni(NO_3)_2 \cdot 6H_2O] + 4[Al(NO_3)_3 \cdot 9H_2O] + 5C_6H_8O_7 + 2HNO_3 = 2NiAl_2O_4 + 9N_2 + 30CO_2 + 69H_2O.$$

The initial components were introduced into combustion mixtures in a stoichiometric ratio. The experimental methodology and the devices used were described in Part 1 [1].

The decoding of the XCP diffractograms was carried out on the JCPDS Cards nos. 10-0425 and 29-0063 for γ-Al_2O_3; 46-1212 for α-Al_2O_3. The diffraction peaks at 19.5, 31.7, 37.5, 45.3, 60.2, and 65.8° correspond to the (111), (220), (311), (222), (400), (511), and (440) planes of $NiAl_2O_4$ and are in excellent agreement with JCPDS Card no. 78-1601 and PDF nos. 65-3102, 81-0718.

RESULTS

All the studied reactions proceeded in a self-propagating mode due to short-term local external heating of the prepared gel.

The XCP (A) diffractograms in Fig. 2 showed that at the stoichiometric ratio of the initial components, the first signs of the crystalline phase appearance in the form of γ-Al_2O_3 in the primary X-ray amorphous product (Fig. 2, *a*) were detected after heat treatment at 700 °C (Fig. 2, *b*). The product annealed at 900 °C fully corresponded to the γ-form (Fig. 2, *c*). The higher temperature treatment (1100 °C) made it possible to obtain single-phase corundum α-Al_2O_3 (Fig. 2, *d*).

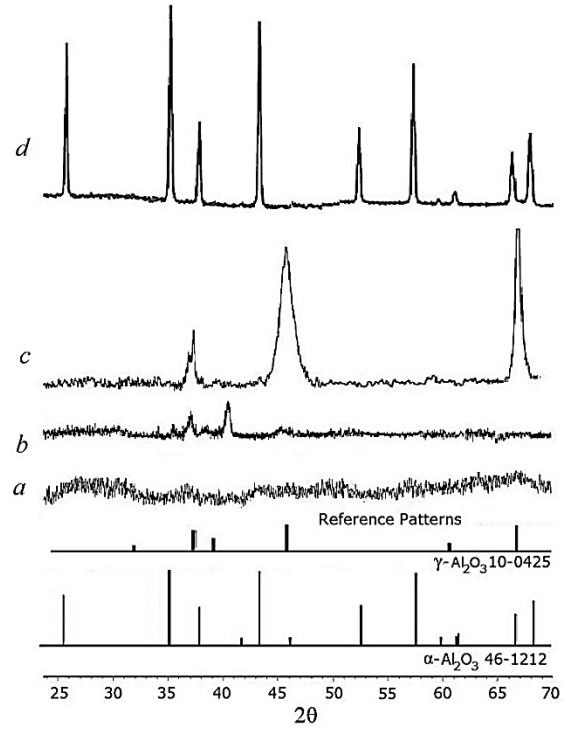

Рис. 2. РФА ПГК (А) после отжига при 500 (*a*), 700 (*b*), 900 (*c*) и 1100 °С (*d*)

Fig. 2. XRD patterns of XCP (A) annealed at 500 (*a*), 700 (*b*), 900 (*c*), and 1100 °C (*d*)

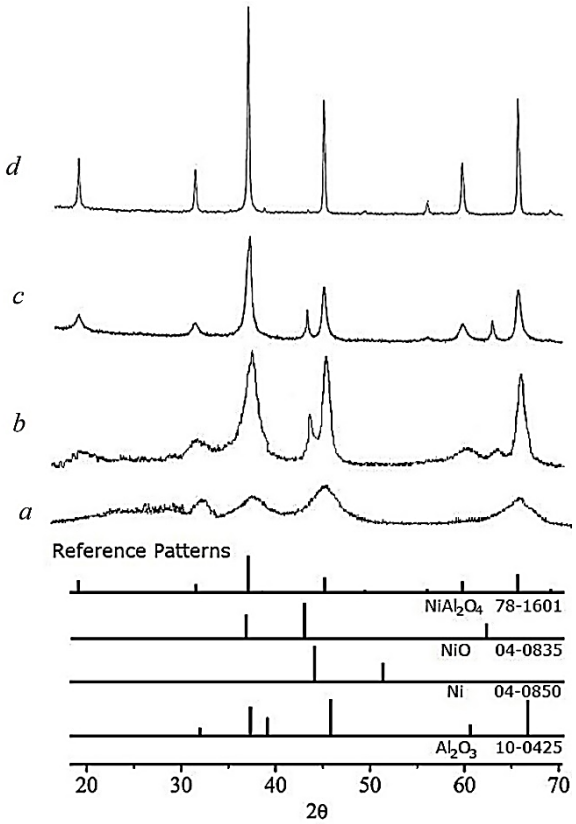

Рис. 3. РФА ПГК (NA) без отжига (*a*) и после отжига при 500 (*b*), 900 (*c*), 1100 °С (*d*)

Fig. 3. XRD patterns of XCP (NA) as-prepared (*a*) and annealed at 500 (*b*), 900 (*c*), 1100 °C (*d*)

In contrast to XCP (A), weak blurred reflexes were detected immediately after combustion on the diffractogram of the mixed product (XCP (NA)) (Fig. 3, *a*). Annealing at 500 °C and above led to the distinct appearance of crystalline spinel signs (Fig. 3, *b*-*c*). At the same time, under these conditions, peaks characteristic of NiO were also manifested, which disappeared during further high-temperature treatment (1100 °C) (Fig. 3, *d*). Nickel metal in XCP (NA), unlike XCP (N) [1], was not detected. The final product was pure spinel $NiAl_2O_4$.

Temperature measurements using an infrared pyrometer during combustion (Fig. 4) made it possible to establish its maximum values T_{max} for XCP (A) and XCP (NA), equal to 429 (curve *2*) and 468 °C (curve *3*), respectively. (For XCP (N), T_{max} was in the interval between these values (curve *1*) and amounted to 447 °C [1]). The difference in the course of the obtained dependencies was manifested only in the different rate of temperature rise up to ~300 °C.

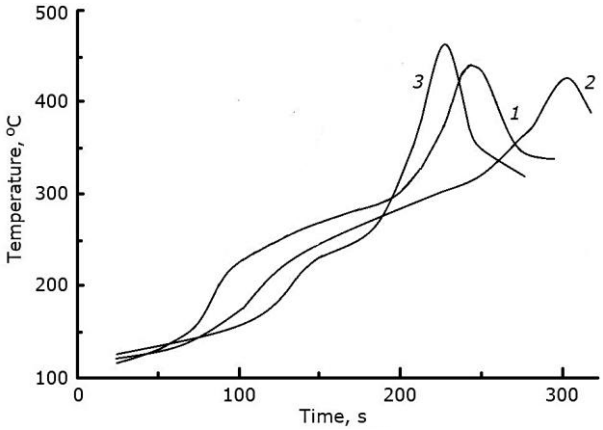

Рис. 4. Изменение температуры во время горения ПГК (N) (*1*), ПГК (А) (*2*), ПГК (NA) (*3*)

Fig. 4. Time-temperature profile of XCP (N) (*1*), XCP (A) (*2*), XCP (NA) (*3*) combustion

The nature of thermal dependencies (TG, DSC) for the studied XCPs was basically identical (Figs. 5, 6). The presence of clearly pronounced exothermic effects testified to an incomplete redox reaction in the combustion process proper. The maximum temperatures, as noted earlier [1, 20], were close to those measured with a pyrometer: 437 (Fig. 5) and 429 °C (Fig. 4, curve *2*), 471 °C (Fig. 6), and 468 °C (Fig. 4, curve *3*). Mass-spectral (MS) curves taken online (Figs. 5, 6) showed a predominant release of gaseous products that corresponded to the redox equations given above: H_2O, N_2, CO_2. Part of the nitrogen was broken off in the forms of NO and NO_2. Basing on these products and literature data [37, 38], it was possible to assume the course of reactions according to the following schemes:

$$Ni(NO_3)_2\cdot 6H_2O \xrightarrow{54\ ^\circ C} Ni(NO_3)_2\cdot 4H_2O \xrightarrow{85,4\ ^\circ C} \xrightarrow{85,4\ ^\circ C} Ni(NO_3)_2\cdot 2H_2O \quad (a)$$

$$Ni(NO_3)_2\cdot 2H_2O = NiO + NO_2 + NO + O_2 + 2H_2O \quad (b)$$

$$Al(NO_3)_3\cdot 9H_2O \xrightarrow{130\ ^\circ C} Al(NO_3)_3 \xrightarrow{200\ ^\circ C} \xrightarrow{200\ ^\circ C} 1/2Al_2O_3 + 3/2NO_2 + 3/2NO + 3/2O_2 \quad (c)$$

$$Ni(NO_3)_2\cdot 2H_2O + C_6H_8O_7 \rightarrow Ni + NiO + NO_2 + NO + N_2 + CO_2 + H_2O + O_2 \quad (d)$$

$$6[Al(NO_3)_3\cdot 9H_2O] + 5C_6H_8O_7 = 3Al_2O_3 + 9N_2 + 30CO_2 + 74H_2O \quad (e)$$

$$2[Ni(NO_3)_2\cdot 6H_2O] + 4[Al(NO_3)_3\cdot 9H_2O] + 5C_6H_8O_7 + 2HNO_3 = 2NiAl_2O_4 + 9N_2 + 30CO_2 + 69H_2O \quad (f)$$

$$Ni + O_2 = NiO + 1/2O_2 \quad (g)$$

$$C_6H_8O_7 = C_5H_4O_3\ (\text{citraconic/itaconic anhydride}) + CO_2 + 2H_2O \quad (h)$$

At the Al_2O_3 interface:

$$2Al_2O_3 + Ni^{2+} = NiAl_2O_4 + 2Al^{3+} + 2O^{2-} \quad (i)$$

At the NiO interface:

$$2NiO + 2Al^{3+} + 2O^{2-} = NiAl_2O_4 + Ni^{2+} \quad (j)$$

Similar to the IR spectrum of XCP (N) [1], the spectra for XCP (A) and XCP (NA) shown in Fig. 7 indicated that the redox reaction was not completed due to the presence of nitrate group residues (~1385-1383, ~1630 cm^{-1}), carboxyl groups (1642-1615 cm^{-1} для ν_{as}(C-O)) with the superimposition of adsorbed water vibrations 1454-1400 cm^{-1} for ν_s(COO) and $\delta(CH_3)$. The band 1088 cm^{-1} (Fig. 7, *c*) and the inflection at 1082 cm^{-1} (Fig. 7, *b*) could be attributed to the M-OH deformation vibrations, as well as the Al–O–C bond [10]. Vibrations of M-O bonds absorbed in the region of 800-450 cm^{-1}. The stretched set of absorption bands in the region of about 520 cm^{-1} (Fig. 7, *a*) could indicate Al-O bonds in the γ-phase [39]. Bands 570-500 and 800-670 cm^{-1} related to vibrations of octahedral AlO_6 and tetrahedral AlO_4 groups, respectively. In addition, the 570-470 cm^{-1} band could be attributed to Ni-O communication vibrations [35, 40]. Based on this, it could be assumed that the product formed as a result of combustion (as-prepared and after annealing) was a partially inverted spinel in a similar way [41], in which Al^{3+} ions are in both octahedral and tetrahedral positions. The characteristic frequencies of the Al–O–Ni vibrations (450-850 cm^{-1}) also indicated the formation of a spinel structure $NiAl_2O_4$ [24]. In [42], bands 715, 600, 495, and 447 cm^{-1} were indicated, which were characteristic of symmetrical stretching, bending, and symmetrical stretching vibrations of Ni–O, Al–O, and Ni–O–Al bonds in tetrahedral and octahedral positions.

Figs. 8, *a*, *b* show agglomerated particles of XCPs (NA) with a size of 100 to 700 nm.

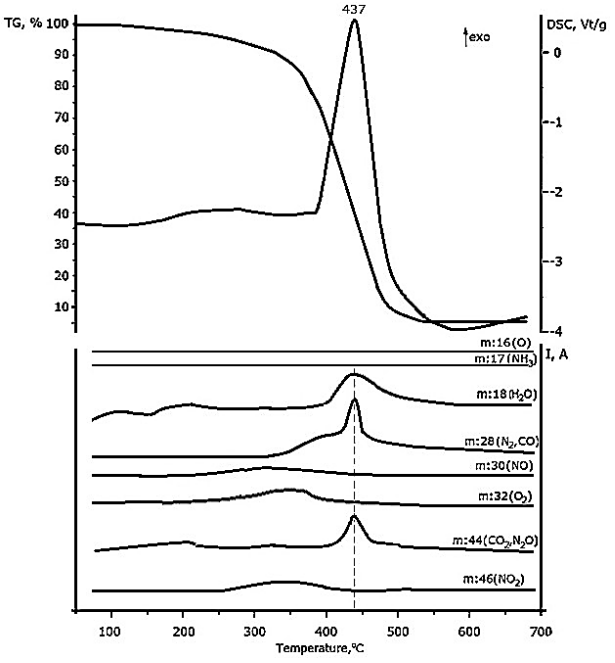

Рис. 5. ТГ/ДСК и масс-спектральные кривые для ПГК (А)
Fig. 5. TG/DSC/MS curves for XCP (A)

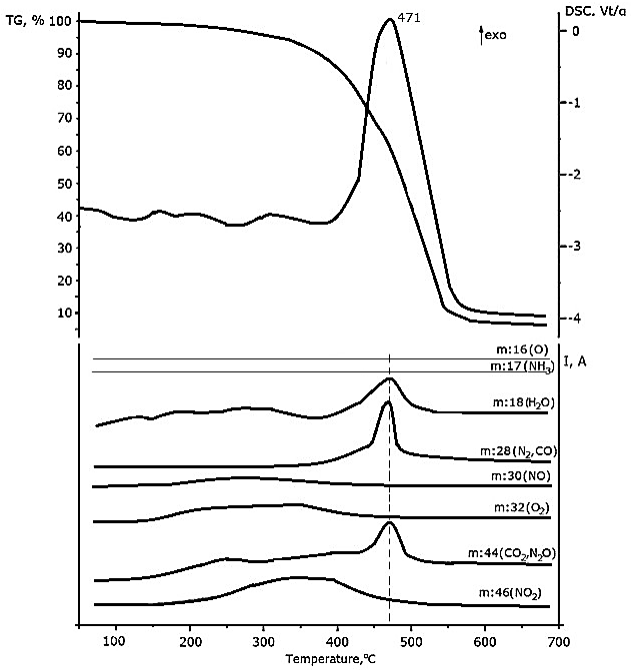

Рис. 6. ТГ/ДСК и масс-спектральные кривые для ПГК (NA)
Fig. 6. TG/DSC/MS curves for XCP (NA)

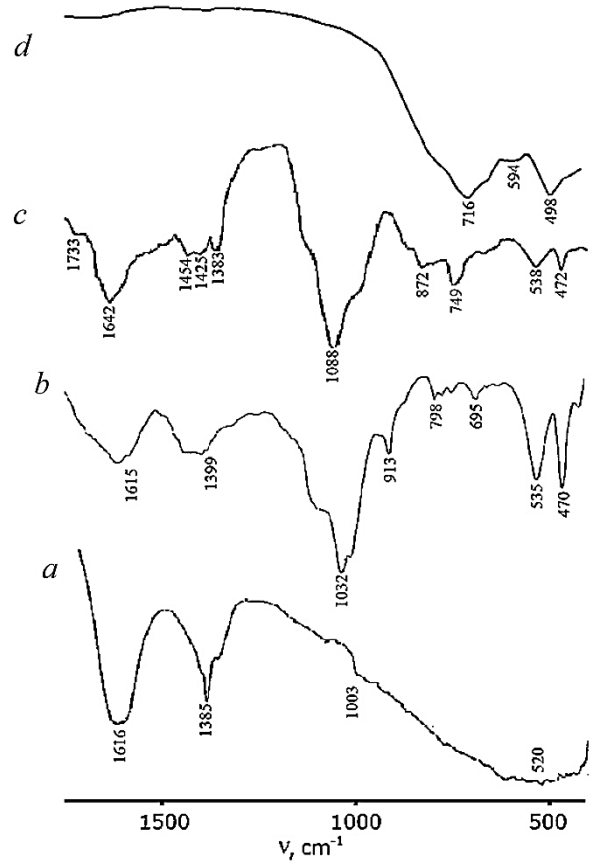

Рис.7. ИК спектры ПГК (А) (*a*) и ПГК (NA) (*b-d*) без отжига (*b*) и после отжига при 500 °С (*a, c*) и 1100 °С (*d*)
Fig. 7. IR spectra of XCP (A) and XCP (NA) as-prepared (*b*) and annealed at 500 °C (*a, c*) and 1100 °C (*d*)

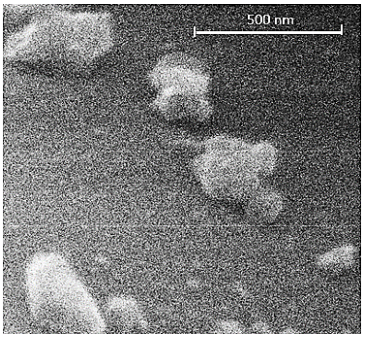

a

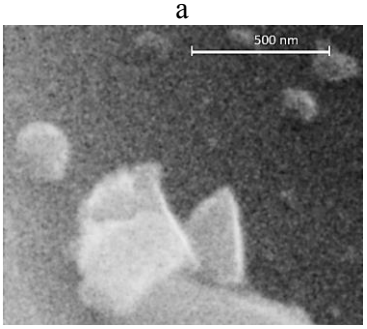

b

Рис. 8. СЭМ-изображения ПГК (NA) без отжига (*a*) и после отжига при 700 (*b*)
Fig. 8. SEM images of XCPs (NA) as-prepared (*a*) and after annealing at 700 (*b*)

The specific surface area (S_{BET}) obtained by low-temperature nitrogen adsorption as well as the equivalent sizes of d_{BET} crystallites for combustion products are shown in the Table. For comparison, data are presented for as-prepared XCP and annealed products, including the data obtained by us [20] for the combustion of XCP (A) with succinic acid (SA) as fuel.

The equivalent sizes of crystallites were calculated according to the equation:

$$d_{BET} = 6000/(\rho \cdot S_{BET}),$$

where ρ is the true density of the corresponding substance, g/cm^3.

Таблица

Удельная площадь поверхности и размеры кристаллитов для продуктов горения

***Table*. Specific surface area and crystallite dimensions for combustion products**

Product	Annealing temperature, °C	S_{BET}, m^2/g	d_{BET}, nm	ρ, g/cm^3
XCP (A) with CA	–	168 ± 20	9.7	
	700	136 ± 12	12	3.68 (γ)
	1100	38 ± 3	40	3.98 (α)
XCP (A) with SA [20]	700	117 ± 5	14	3.68 (γ)
	1100	21 ± 3	72	3.98 (α)
XCP (N) with CA	–	72 ± 4	11	7.45
	700	59 ± 3	14	7.45
XCP (NA) with CA	–	85 ± 10	16	4.50
	700	74 ± 8	18	4.50

The data obtained indicated a slight decrease in the specific surface area (by 13-19%) and an increase in the size of crystallites (by 13-27%), as well as their agglomerates (Fig. 8) as a result of heat treatment at 700 °C. Only a higher temperature (1100 °C) led to a significant reduction in the interfacial surface (4-5 times).

Subsequently, the synthesized XCP (A) was used for the synthesis of nickel-aluminate spinel, and the kinetics of solid-phase reactions of $NiAl_2O_4$ formation with the participation of XCPs was studied.

CONCLUSION

Xerogel combustion products (XCPs) were obtained from a mixture of aluminum nitrate and citric acid (XCP (A)) and from a mixture of aluminum and nickel nitrates with the addition of citric acid (XCP (NA)) for the subsequent synthesis of nickel aluminate spinel. With the help of X-ray diffraction, it was shown that the as-prepared XCP(A) was amorphous. After heat treatment at 700-900 °C, a crystalline phase in the form of γ-Al_2O_3 was detected, which at 1100 °C turned into single-phase corundum α-Al_2O_3. Signs of $NiAl_2O_4$

were manifested in as-prepared XCP (NA). Single-phase spinel (without NiO impurity) was obtained as a result of annealing at 1100 °C.

The maximum values of the combustion temperature have been established: 429 °C for XCP (A) and 468 °C for XCP (NA). The composition of gaseous products released in redox reactions was determined. The IR spectra of as-prepared XCPs and after annealing were analyzed. The specific surface area values as well as the equivalent sizes of d_{BET} crystallites for combustion products are calculated.

ACKNOWLEDGEMENTS

The work was carried out within the framework of the state assignment for the implementation of research work (Topic No. FZZW-2024-0004). The study was carried out using the resources of the Center for Collective Use of Scientific Equipment of ISUCT.

The authors declare the absence of a conflict of interest warranting disclosure in this article.

Работа выполнена в рамках государственного задания на выполнение НИР (Тема № FZZW-2024-0004). Исследование выполнено с использованием ресурсов Центра коллективного пользования научной аппаратурой ИГХТУ.

Авторы заявляют об отсутствии конфликта интересов, требующего раскрытия в данной статье.

REFERENCES
ЛИТЕРАТУРА

1. **Филатова Н.В., Артюшин А.С., Косенко Н.Ф., Павлова К.А., Никандрова А.Г.** Три варианта синтеза никельалюми-натной шпинели с использованием продуктов горения ксерогелей. Часть 1. *Изв. вузов. Химия и хим. технология*. 2026. Т. 69. Вып. 5. С. 74-81. **Filatova N.V., Artyushin A.S., Kosenko N.F., Pavlova K.A., Nikandrova A.G.** Three variants of nickel aluminate spinel synthesis using xerogel combustion products. Part 1. *ChemChemTech [Izv. Vyssh. Uchebn. Zaved. Khim. Khim. Tekhnol.]*. 2026. V. 69. N 5. P. 74-81. DOI: 10.6060/ivkkt.20266905.6993.
2. **Kingsley J.J., Patil K.C.** A novel combustion process for the synthesis of fine particle α-alumina and related oxide materials. *Mater. Lett.* 1988. V. 6, N 11–12. P. 427-432. DOI: 10.1016/0167-577X(88)90045-6.
3. **Ianoș R., Muntean E., Băbuță R., Lazău R., Păcurariu C., Bandas C.** Combustion synthesis of pink chromium-doped alumina with excellent near-infrared reflective properties. *Ceram. Int.* 2017. V. 43. P. 2568–2572. DOI: 10.1016/j.ceramint.2016.11.061.
4. **Jolly B.M., Ravi S.K., Ipe S., Bhattacharya S.S.** Effect of Process Parameters on the Characteristics of Nanocrystalline Alumina Particles Synthesized by Solution Combustion Process. *Trans. Indian Inst. Met.* 2015. V. 68 (Suppl. 2). P. 147–151. DOI: 10.1007/s12666-015-0534-8.
5. **Prashanth P.A., Raveendra R.S., Hari Krishna R., Ananda S., Bhagya N.P., Nagabhushana B.M., Lingaraju K., Raja Naika H.** Synthesis, characterizations, antibacterial and photoluminescence studies of solution combustion-derived α-Al_2O_3 nanoparticles. *J. Asian Ceram. Socs.* 2015. V. 3. N 3. P. 345-351. DOI: 10.1016/j.jascer.2015.07.001.
6. **Roque-Ruiz J.H., Reyes-López S.Y.** Synthesis of α-Al_2O_3 nanopowders at low temperature from aluminum formate by combustion process. *J. Mater. Sci. Eng.* 2016. V. 6. P. 1000305. DOI: 10.4172/2169-0022.1000305.
7. **Behera P.S., Bhattacharyya S.** Thermal decomposition, phase evolution and morphology study of combustion synthesized alumina powder – Influence of precursor pH. *Mater. Chem. Phys.* 2021. V. 259. P. 124030. DOI: 10.1016/j.matchemphys.2020.124030.
8. **Zhuravlev V.D., Bamburov V.G., Beketov A.R., Perelyaeva L.A., Baklanova I.V., Sivtsova O.V., Vasil'ev V.G., Vladimirova E.V., Shevchenko V.G., Grigorov I.G.** Solution combustion synthesis of α-Al_2O_3 using urea. *Ceram. Int.* 2013. V. 39. P. 1379–1384. DOI: 10.1016/j.ceramint.2012.07.078.
9. **Salehi M., Arabsarhangi E.** Solution combustion synthesis using Schiff-base aluminum complex without fuel and optical property investigations of alumina nanoparticles. *Int. Nano Lett.* 2015. V. 5. P. 141–146. DOI: 10.1007/s40089-015-0147-6.
10. **Salem S., Salem A., Parni M.H., Jafarizad A.** Facile and rapid auto-combustion synthesis of nano-porous γ-Al_2O_3 by application of hexamethylenetetramine in fuel composition. *J. Phys. Chem. Solids*. 2018. V. 117. P. 86-93. DOI: 10.1016/j.jpcs.2018.02.019.
11. **Patil S.D., Sherikar P., Sherikar B.N.** Synthesis of γ-Alumina by Solution Combustion Method using Mixed Fuel Approach (Urea+Citric Acid Fuel). *IJSRD – Int. J. Sci. Res. Develop.* 2016. V. 4(08). P. 616-618.
12. **Mandić V., Kurajica S., Mužina K., Brleković F., Munda I.K.** Tailoring thermal development of gamma alumina sorbents material using combustion synthesis: the effect of amino acids (G, A, N) and equivalence ratio. *J. Therm. Anal. Calorim.* 2020. V. 142. P. 1681–1691. DOI: 10.1007/s10973-020-10258-0.
13. **Gupta B., Pujar P., Mal S.S., Gupta D., Mandal S.** Retention of high dielectric constant sodium beta alumina via solution combustion: Role of aluminum ions complexation with fuel. *Ceram. Int.* 2018. V. 44. P. 1500–1511. DOI: 10.1016/j.ceramint.2017.10.061.
14. **Shi J., Hong Y., Zhu C.** Effect of Chromium on Electrochemical and Mechanical Properties of Beta-Al_2O_3 Solid Electrolyte Synthesized Via a Citrate-Nitrate Combustion Method. *Crystals*. 2020. V. 10. P. 987. DOI: 10.3390/cryst10110987.
15. **Rajaeiyan A., Bagheri-Mohagheghi M.M.** Comparison of Urea and Citric Acid Complexing Agents and Annealing Temperature Effect on the Structural Properties of γ- and α-Alumina Nanoparticles Synthesized by Sol-Gel Method. *Adv. Mater. Sci. Eng.* 2013. V. 2013. P. 791641. DOI: 10.1155/2013/791641.
16. **Романовский В.И., Хорт А.А., Подболотов К.Б., Сдобняков Н.Ю., Мясниченко В.С., Соколов Д.Н.** Одностадийный синтез полиметаллических наночастиц в воздушной среде. *Изв. вузов. Химия и хим. технология.* 2018. Т. 61. Вып. 9-10. С. 42-47. **Romanovskii V.I., Khort A.A., Podbolotov K.B., Sdobnyakov N.Y., Myasnichenko V.S., Sokolov D.N.** One-step synthesis of polymetallic nanoparticles in air invironment. *ChemChemTech [Izv. Vyssh. Uchebn. Zaved. Khim. Khim. Tekhnol.]*. 2018. V. 61. N 9-10. P. 42-47 (in Russian). DOI: 10.6060/ivkkt.20186109-10.5867a.
17. **Frikha K., Limousy L., Bouaziz J., Bennici S., Chaari K., Jeguirim M.** Elaboration of alumina-based materials by solution combustion synthesis: A review. *C. R. Chimie*. 2019. V. 22. P. 206-219. DOI: 10.1016/j.crci.2018.10.004.
18. **Krishna Ch.N.S., Venu M.** Synthesis of alumina nanopowder using mixed fuel by solution combustion approach.

IJRET: Int. J. Res. Eng. Technol. 2016. V. 05 N 13. DOI: 10.15623/IJRET.2016.0525030

19. **Mallappa B.K., Kamble P.G.** Solution combustioning of alumina using combined urea+ camphor fuel. *Int. J. Latest Trends Eng. Technol.* 2021. V. 16. N 1. P. 026-031. DOI: 10.21172/1.164.04.
20. **Филатова Н.В., Артюшин А.С., Косенко Н.Ф.** Синтез и характеристика продукта горения алюмооксидно-сукцинатного ксерогеля. *Рос. хим. ж. (Ж. Рос. хим. об-ва).* 2025. Т. LXIX. №2. С. 22-29. **Filatova N.V., Artyushin A.S., Kosenko N.F.** Synthesis and characterization of the combustion product of aluminum-succinate xerogel. *Ros. Khim. Zh.* 2025. V. 69. N 2. P. 22-29 (in Russian). DOI: 10.6060/rcj.2025692.4.
21. **Филатова Н.В., Косенко Н.Ф., Артюшин А.С., Малоиван М.С., Зонина И.И., Власенков А.С.** Реакционная способность алюмооксидных прекурсоров для твердофазного образования шпинели $MgAl_2O_4$. *Изв. вузов. Химия и хим. технология.* 2024. Т. 67. Вып. 12. С. 15-24. **Filatova N.V., Kosenko N.F., Artyushin A.S., Maloivan M.S., Zonina I.I., Vlasenkov A.S.** Reactivity of aluminum oxide precursors for solid-phase formation of $MgAl_2O_4$ spinel. *ChemChemTech [Izv. Vyssh. Uchebn. Zaved. Khim. Khim. Tekhnol.].* 2024. V. 67. N 12. P. 15-24. DOI: 10.6060/ivkkt.20246712.7152.
22. **Han M., Wang Z., Xu Y., Wu R., Jiao S., Chen Y., Feng S.** Physical properties of $MgAl_2O_4$, $CoAl_2O_4$, $NiAl_2O_4$, $CuAl_2O_4$, and $ZnAl_2O_4$ spinels synthesized by a solution combustion method. *Mater. Chem. Phys.* 2018. V. 215. P. 251–258. DOI: 10.1016/j.matchemphys.2018.05.029.
23. **Jayasree S., Manikandan A., Antony S.A., Mohideen A.U., Barathiraja C.** Magneto-optical and catalytic properties of recyclable spinel $NiAl_2O_4$ nanostructures using facile combustion methods. *J. Supercond. Novel Magnet.* 2016. V. 29. P. 253–263. DOI: 10.1007/s10948-015-3249-5.
24. **Ragupathi C., Vijaya J.J., Kennedy L.J.** Preparation, characterization and catalytic properties of nickel aluminate nanoparticles: A comparison between conventional and microwave method. *J. Saudi Chem. Soc.* 2017. V. 21. P. S231–S239. DOI: 10.1016/j.jscs.2014.01.006.
25. **Zygmuntowicz J., Miazga A., Kamiński Ł., Konopka K.** Synthesis and Characterization of Nickel Aluminate Spinel ($NiAl_2O_4$) Prepared from the Equilibrium Mixture of Al_2O_3 and NiO. *Appl. Mechan. Mater.* 2015. V. 797. P. 391–399. DOI: 10.4028/www.scientific.net/amm.797.391.
26. **Mahi K., Benabdellah G., Kada E.Z.O., Trari M.** Preparation and spectroscopic study of nanosized aluminate spinels Al_2XO_4 (X = Cd, Ni and Co) synthesized by solution combustion technique. *Indian J. Phys.* 2024. V. 98. N 9. P. 3229-3236. DOI: 10.1007/s12648-024-03096-5.
27. **Frikha K., Bennici S., Bouaziz J., Chaari K., Limousy L.** Influence of the Fuel/Oxidant Ratio on the Elaboration of Binary Oxide Catalyst by a Microwave-Assisted Solution Combustion Method. *Energies*. 2020. V. 13. N 12. P. 3126. DOI: 10.3390/en13123126.
28. **Gao Y., Meng F., Cheng Y., Li Z.** Influence of fuel additives in the urea-nitrates solution combustion synthesis of Ni-Al_2O_3 catalyst for slurry phase CO methanation. *Appl. Catal. A.* 2017. V. 534. P. 12–21. DOI: 10.1016/j.apcata.2017.01.016.
29. **Kurmashov P.B., Ukhina A.V., Manakhov A., Ishchenko A.V., Maksimovskii E.A., Bannov A.G.** Solution Combustion Synthesis of Ni/Al_2O_3 Catalyst for Methane Decomposition: Effect of Fuel. *Appl. Sci.* 2023. V. 13. P. 3962. DOI: 10.3390/app13063962.
30. **Nasiri H., Vahdati Khaki J., Shahtahmassebi N.** Effect of alumina percentage on size and superparamagnetic properties of Ni-Al_2O_3 nanocomposite synthesized by solution combustion. *Mater. Des.* 2016. V. 109. P. 476–484. DOI: 10.1016/j.matdes.2016.07.101.
31. **Ponugoti P.V., Pathmanathan P., Rapolu J., Gomathi A., Janardhanan V.M.** On the stability of Ni/γ-Al_2O_3 catalyst and the effect of H_2O and O_2 during biogas reforming. *Appl. Catal. A: Gen.* 2023. V. 651. P. 119033. DOI: 10.1016/j.apcata.2023.119033.
32. **Medeiros R.L.B.A., Figueredo G.P., Macedo H.P., Oliveira Â.A.S., Rabelo-Neto R.C., Melo D.M.A., Braga R.M., Melo M.A.F.** One-pot microwave-assisted combustion synthesis of Ni-Al2O3 nanocatalysts for hydrogen production via dry reforming of methane. *Fuel.* 2021. V. 287. P. 119511. DOI: 10.1016/j.fuel.2020.119511.
33. **Farahani M.D., Valand J., Mahomed A.S., Friedrich H.B.** A Comparative Study of NiO/Al_2O_3 Catalysts Prepared by Different Combustion Techniques for Octanal Hydrogenation. *Catal. Lett.* 2016. V. 146. P. 2441–2449. DOI: 10.1007/s10562-016-1858-7.
34. **Heydari A., Ahmadpour A., Nayebzadeh H., Saghatoleslami N., Azmoon A.-H.** Fabrication of sulfated spinel nickel aluminate for biofuel production: influence of Ni/Al ratio on its activity. *Appl. Nanosci.* 2020. V. 10. P. 1981–1995. DOI: 10.1007/s13204-020-01311-3.
35. **Gholami T., Salavati-Niasari M., Salehabadi A., Amiri M., Shabani-Nooshabadi M., Rezaie M.** Electrochemical hydrogen storage properties of $NiAl_2O_4$/NiO nanostructures using TiO_2, SiO_2 and graphene by auto-combustion method using green tea extract. *Renew. Energy.* 2018. V. 115. P. 199-207. DOI: 10.1016/j.renene.2017.08.037.
36. **Tungatarova S.A., Manabayeva A.M., Abilmagzhanov A.Z., Baizhumanova T.S., Malgazhdarova M.K.** Application of Catalysts Prepared by Solution Combustion Synthesis in Dry Reforming of Methane. *Molecules*. 2025. V. 30. P. 4575. DOI: 10.3390/molecules30234575.
37. **Thoda O., Xanthopoulou G., Vekinis G., Chroneos A.** Parametric Optimisation of Solution Combustion Synthesis Catalysts and Their Application for the Aqueous Hydrogenation of Maleic Acid. *Catal. Lett.* 2018. V. 148. P. 764–778. DOI: 10.1007/s10562-017-2279-y.
38. **Wyrzykowski D., Hebanowska E., Nowak-Wiczk G., Makowski M., Chmurzyński L.** Thermal behaviour of citric acid and isomeric aconitic acids. *J. Therm. Anal. Calorim.* 2011. V. 104. P. 731–735. DOI: 10.1007/s10973-010-1015-2.
39. **Maĉedo M.J.F., Osava C.C., Bertran C.A.** Sol-gel synthesis of transparent alumina gel and gamma alumina by urea hydrolysis of aluminum nitrate. *J. Sol-Gel Sci. Technol.* 2004. V. 30. P. 135. DOI: 10.1023/B:JSST.0000039497.46154.8f.
40. **Филатова Н.В., Косенко Н.Ф., Денисова О.П., Садкова К.С.** Физико-химическое изучение каолина месторождения Журавлиный Лог. Часть 1. *Изв. вузов. Химия и хим. технология.* 2022. Т. 65. Вып. 8. С. 85-93. **Filatova N.V., Kosenko N.F., Denisova O.P., Sadkova K.S.** The physicochemical investigation of the Zhuravliny Log kaolin. Part 1. *ChemChemTech [Izv. Vyssh. Uchebn. Zaved. Khim. Khim. Tekhnol.].* 2022. V. 65. N 8. P. 85-93. DOI: 10.6060/ivkkt.20226508.6656.
41. **Filatova N.V., Kosenko N.F., Denisova O.P.** The Regulation of Spinel Precursors Reactivity by Means of a Mechanical and a Microwave Treatment. *Russ. J. Phys. Chem. A.* 2022. V. 96. N 6. P. 1147–1154. DOI: 10.1134/S0036024422060085.
42. **Tangcharoen T., T-Thienprasert J., Kongmark C.** Effect of calcination temperature on structural and optical properties of MAl_2O_4 (M = Ni, Cu, Zn) aluminate spinel nanoparticles. *J. Adv. Ceram.* 2019. V. 8. N 3. P. 352–366. DOI: 10.1007/s40145-019-0317-5.

Поступила в редакцию (Received) 17.03.2026
Принята к опубликованию (Accepted) 25.03.2026